Compression Strength Size Effect on Carbon-PEEK Fiber Composite Failing by Kink Band Propagation

Kim, Jang-Ho*

ABSTRACT

The effect of structure size on the nominal strength of unidirectional fiber-polymer composites, failing by propagation of a kink band with fiber microbuckling, is analyzed experimentally and theoretically. Tests of novel geometrically similar carbon-PEEK specimens, with notches slanted so as to lead to a pure kink band (without shear or splitting cracks), are conducted. The specimens are rectangular strips of widths 15.875, 31.75, and 63.5 mm (0.625, 1.25 and 2.5 in and gage lengths 39.7, 79.375 and 158.75 mm (1.563, 3.125 and 6.25 in.). They reveal the existence of a strong (deterministic, non-statistical) size effect. The doubly logarithmic plot of the nominal strength (load divided by size and thickness) versus the characteristic size agrees with the approximate size effect law proposed for quasibrittle failures in 1983 by Bazant. This law represents a gradual transition from a horizontal asymptote, representing the case of no size effect (characteristic of plasticity or strength criteria), to an asymptote of slope -1/2 (characteristic of linear elastic fracture mechanics, LEFM). The size effect law for notched specimens permits easy identification of the fracture energy of the kink bandand the length of the fracture process zone at the front of the band solely from the

* KCI Member, Assistant Professor, Dept. of Civil and Environmental Engineering, Sejong University, KOREA

measurements of maximum loads. Optimum fits of the test results by the size effect law are obtained, and the size effect law parameters are then used to identify the material fracture characteristics, particularly the fracture energy and the effective length of the fracture process zone. The results suggest that composite size effect must be considered in strengthening existing concrete structural members such as bridge columns and beams using a composite retrofitting technique.

Keywords : carbon-PEEK composite, size effect, microbuckling, delamination fracture, splitting-shear crack, kink band crack, quasibrittle failure, fracture process zone, stress intensity factor, energy release rate, compression strength, characteristic size, slanted notch.

1. Introduction

In the early 1980's it became clear that the size effect on the nominal strength of quasi-brittle materials failing after large stable crack growth is caused principally by energy release[3] and cannot be explained by Weibull-type statistics of random micro-defects. Size effects caused by energy release into a finite-size fracture process zone (damage localization zone) have been extensively demonstrated and mathematically described for concrete, mortar, rocks, ceramics and sea ice. Description of such a size effect requires an energy analysis of fracture mechanics. At present, all the textbooks and practical procedures for fiber composites characterize the failure in terms of strength or plasticity type criteria, which are inherently incapable of capturing the size effect. Recently, though, the existence of size effect has been demonstrated by tests of notched orthotropic and quasi-isotropic carbon-epoxy laminates under tensile (Mode I) loading[7]. Since a currently popular retrofitting technique for strengthening existing concrete structural members such as concrete bridge columns and beams requires the usage of composite material, the size effect of composite must be further studied.

The present study will focus attention on the compression failure of unidirectionally reinforced fiber composites. This is a particularly complex type of material failure, which can involve two distinct mechanisms: (1) delamination fracture, and (2) axial splitting-shear cracks combined with micro-buckling of fibers in a so-called kink band. Only the later mechanism of failure will be considered in this study.

This study, involving specimens that strictly adhere to geometrical similarity, reports experimental results that reveal and confirm the existence a size effect in kink band compression failure and permit approximate calibration of size effect theory. The size effect caused by fracture has recently come to the forefront of attention in the studies of quasibrittle materials, which are characterized by the existence of a sizable fracture process zone at the tip of a macroscopic crack. It has been found that in such materials the size effect is transitional between plasticity (for which there is no size effect) and linear elastic fracture mechanics[3, 4, 9, 10]. Thus the plot of $\log \sigma_N$ versus $\log D$ is a smooth curve approaching at very small sizes a horizontal asymptote corresponding to

plasticity and at very large sizes an inclined asymptote of slope, -0.5, corresponding to linear elastic fracture mechanics. Such a size effect must generally occur whenever the load-deflection diagram does not have a yield plateau after the maximum load is reached, provided that the geometrically nonlinear effects of buckling are absent. Therefore, a size effect of this type should be expected also for fiber composite laminates. The purpose of this paper is to verify this proposition, describe the size effect quantitatively and utilize measurements of the size effect for determining the material fracture characteristics. Note that geometrically similar structures of different sizes are compared and the cracks at maximum load are also geometrically similar.

It must be emphasized that this study deals only with the size effect for constant thickness of the laminate and for the same layup. If the thickness is varied, a size effect of different type occurs, which is not investigated here. Also, only the size effect for the same notch tip sharpness is studied, however, for sufficiently small notch tip widths, less than about 1/3 of the spacing of major inhomogeneities, the sharpness effect may be expected to disappear.

2. Size Effect Tests of Notched Specimens

The kink band failure is often combined with axial splitting-shear cracks and delaminations. Such combined failures are difficult to analyze because the contributions of the microbuckling in the kink band and of the shear, splitting and delamination failures are difficult to separate. Therefore, the objective of experimental investigation is aimed at finding the type of fiber composite and the shape of specimen that would lead to a pure kink band failure and does so for even very large sizes.

After experimenting with various types of composites, the carbon fiber composite with a PEEK (poly-ether-ether-ketone) thermoplastic polymer matrix was selected. The advantage of PEEK is that it is less brittle than carbon epoxy composites, which leads to a more stable type of failure. It follows that, if a size effect is revealed in this type of composite, it should exist and be in fact more pronounced in more brittle composites, such as the carbon epoxy composites.

The material used was AS2/APC4 carbon/PEEK obtained in unidirectional prepreg form. Unidirectional laminates were prepared from this prepreg. The properties of the unidirectional lamina at room temperature are provided by the manufacturer and are listed in Table 2.

Table 1 Properties of unidirectional APC-2/AS4 carbon-PEEK.

Property	Value
Fiber volume ratio, V_f	0.61
Ply thickness, t, mm (in.)	0.141 (0.0056)
Longitudinal modulus, E_1, GPa (Msi)	138 (20)
Transverse modulus, E_2, GPa (Msi)	10.2 (1.5)
In-plane shear modulus, G_{12}, GPa (Msi)	5.7 (0.82)
Major Poisson's ratio, ν_{12}	0.30
Longitudinal tensile strength, F_{1t}, MPa (ksi)	2070 (300)
Transverse tensile strength, F_{2t}, MPa (ksi)	86 (13)
Fracture toughness, Mode I G_{1c}, kN/m (lbf/in)	1.7 (9.7)
Fracture toughness, Mode II G_{1c}, kN/m (lbf/in)	2.0 (11.4)

Table 2 Results of compression tests of notched composite laminates of different sizes.

Size	Gauge length cm (in.)	Width cm (in.)	Max. load, P, kN (kips)	Nominal strength, σ_N, MPa (ksi)
Small	3.97 (1.56)	1.61 (0.63)	81.18 (18.25)	372.9 (54.09)
	3.97 (1.56)	1.61 (0.63)	78.20 (17.58)	379.0 (54.97)
	3.97 (1.56)	1.60 (0.63)	112.71 (25.34)	522.2 (75.74)
Medium	7.94 (3.125)	3.27 (1.29)	142.74 (32.09)	347.6 (50.42)
	7.94 (3.125)	3.11 (1.23)	111.24 (25.01)	289.7 (42.01)
	7.94 (3.125)	3.25 (1.28)	116.14 (26.11)	281.2 (40.79)
Large	15.88 (6.25)	6.45 (2.54)	223.91 (50.34)	258.9 (37.55)
	15.88 (6.25)	6.39 (2.52)	263.63 (59.27)	316.7 (45.94)
	15.88 (6.25)	6.34 (2.50)	241.17 (54.22)	282.6 (40.98)

The content of polymer resin in the specimen, supplied by Fiberite, Inc., Orange, California, was 32±3%. The specimens have been molded from 100 plies of sheets 304.8 mm x 304.8 mm (12 in. x 12 in.), 12.7 mm (0.5 in.) thick. The molding was carried out under temperature 390.6 ℃ and pressure 0.69 MPa (0.1 ksi), using the standard time sequence of the curing process. The specimens are cut from the tile according to the desired size. The specimens consisted of three rectangular tiles of the same thickness but different sizes, geometrically similar in the planes of the laminates, with width x gage length = 15.875 x 39.7 mm, 31.75 x 79.375 mm, and 63.5 x 158.75 mm (0.625 x 1.563 in., 1.25 x 3.125 in., and 2.5 x 6.25 in.). Thus the size ratios were 1:2:4.

To exclude the effect of random variation of material strength over the specimen volume (known to cause Weibull-type size effect), the specimens need to be provided with notches. The notches ensure the failure to begin in the desired place, thus preventing the failure to start where the material is statistically weakest.

Normally notches orthogonal to the surface are used in fracture testing. Such notches, however, have been found to lead to failures that begin by an axial splitting-shear crack, which is only later followed by the development of a transversely propagating out-of-plane kink band. The band has been observed in this program, as well as previously by Fleck et al.[13], to be transversely inclined. For this reason, the starter notch was made inclined as shown in Figure 3c, with the same angle as the observed kink band. The proper inclination, found by trial tests to be 25.4 °, has made it possible to eliminate entirely the axial splitting-shear cracks and thus obtain pure kink band failures.

Single edge slanted notch of length $a = 0.3D$ was machined, where D is the specimen width (Figure 1). The notches were machined with diamond bladed band saw up to 95 % of a and the notch tip of 5 % of a with 0.2 mm (0.008 in) diameter diamond-studded wire. Thus, the crack tip radius was 0.1 mm (0.004 in.) in all the specimens. After the specimens had been cut from the molded sheets, they were provided with massive end caps made of 1040 hot rolled steel, to which they are glued by epoxy. The total length of all specimens accounted for the extra length needed to attach end caps. To ensure proper alignment, the end caps were glued only after the specimen had been installed under the

loading platens of the testing machine. The end caps serve not only for applying uniform compressive stress on the cross section of the specimen but offers sufficient confinement at the exposed ends of the specimen to delay the brush, shear failure during the loading.

The photo of test specimens is shown in Figure 3a and their dimensions are shown in Figure 1. They are scaled in two dimensions, the thickness in the third dimension being constant. The specimen dimensions as well as the depth of the notches is scaled in the ratio 1:2:4.

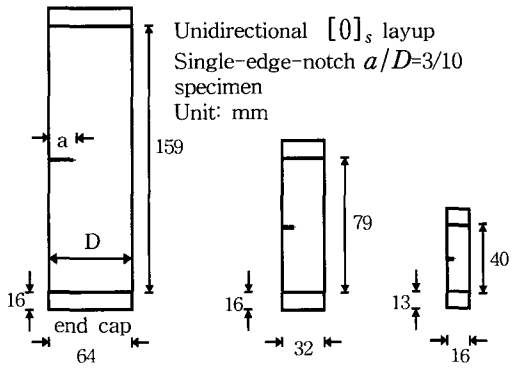

Fig. 1 Geometry of test specimens (units : mm)

All the specimens have been tested under a controlled stroke rate of 1.27×10^{-4} mm/second (5×10^{-6} inch/second). After the kink band had initiated at the notch tip, it was seen to propagate stably on both the front and back sides of the specimen (Figures 2a-d and 3b). The length of the kink band on one side was usually slightly longer than on the other side, but only at the beginning of propagation. The shorter band on one side would soon catch up with the longer band on the opposite side. The maximum load for all the specimens was reached while the kink band extended only 1.0 mm (0.04 in.) from the notch tip shown Figure 3b.

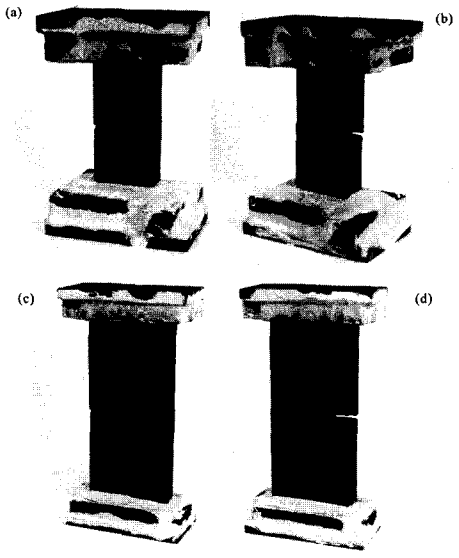

Fig. 2 (a) Front and
(b) back face of medium size specimens after compression
(c) Front and
(d) back face of large size specimens after compression.

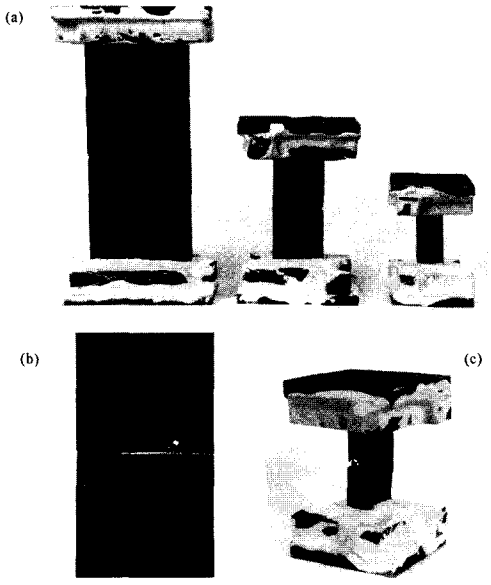

Fig. 3 (a) Comparison of various size specimens
(b) Propagation of kink band crack across the width of large size specimen
(c) Small size specimen with slanted notch

Figures 4a, 5a, and 6a, are applied compressive load versus relative end displacement plots of small, medium, and large specimens and Figures 4b, 5b, and 6b are corresponding stress versus strain plots. For the sake of statistical variation, three tests are done for each specimen size. All curves in Figures 4a, 5a, and 6a except one small size specimen indicate relatively ductile behavior. The curves are linear in the elastic zone and show a significant smooth, nonlinear segment as the peak load is approached. The distinct indication of the peak load where the transition from the elastic to the initiation of damage is continuous and smooth one is due to the ductile characteristic of PEEK. Unlike the brittle failure of fiber epoxy composites[7], carbon fiber reinforced PEEK clearly shows higher ductility. The indirect advantage of the ductile response is that the unique peak load (equivalent to maximum nominal strength) can be measured and better assessment the

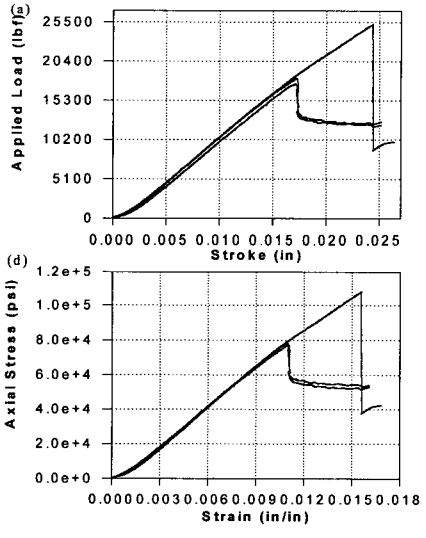

Fig. 4 (a) Axial force versus relative axial displacement of end platens diagram and
(b) Axial stress versus relative axial strain of end platens diagram for small specimens

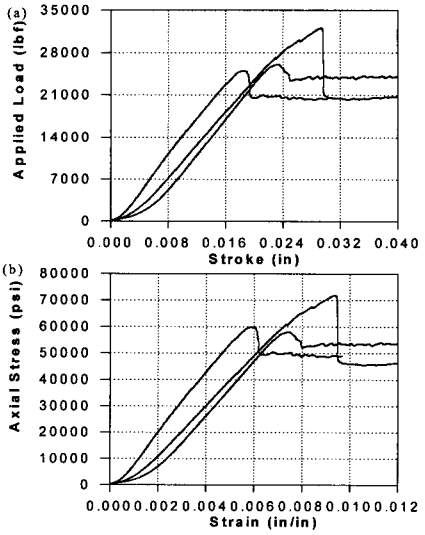

Fig. 5 (a) Axial force versus relative axial displacement of end platens diagram and
(b) Axial stress versus relative axial strain of end platens diagram for medium specimens

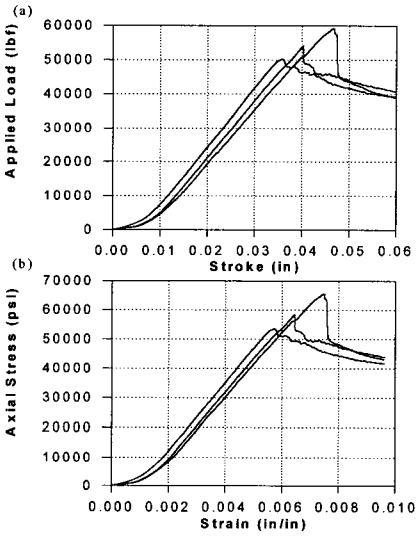

Fig. 6 (a) Axial force versus relative axial displacement of end platens diagram and
(b) Axial stress versus relative axial strain of end platens diagram for large specimens

size effect and other fracture and mechanical properties of the material can be done.

The test results for the notched specimens are summarized in Table 2, in which the

nominal strength is defined as the average stress at failure based on the notched cross section,

$$\sigma_N = \frac{P_{max}}{bD}$$

where,

P_{max} = maximum load measured
b = specimen thickness (12.7 mm)
D = specimen width (chosen as the characteristic dimension)

Figure 7 shows the individual test results in the form of the plot of log σ_N versus log D.

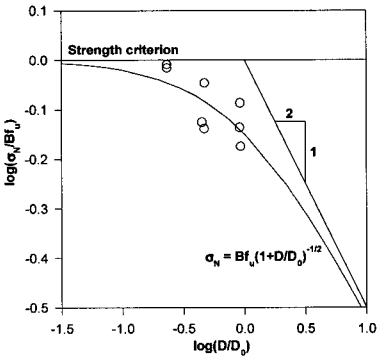

Fig. 7 Size effect measured for unidirectional specimens

If there was no size effect, as currently assumed in design and exhibited by the existing formulas for the maximum load expressed in terms of stress or strain, the plot in Figure 7 would have to be horizontal. Every theory based on plasticity or on critical values of stress or strain would require a horizontal plot. However, the trend is seen to be strongly downward. The downward slope is found to be quite steep and close to the slope that would be predicted for geometrically similar specimens with similar notches by linear elastic fracture mechanics (LEFM), which equals -1/2 and is indicated in the figure. So, despite using a relatively ductile PEEK matrix, the size effect is strong for these, not extremely large, specimens.

The test results exhibit considerable scatter. This is, however, typical of compression failure of fiber composites because of their strong sensitivity to fiber misalignment[12),(14)]. For this reason, the size effect would not have been revealed clearly if the size range were less than 1:4. The present size range of 1:4 appears just about the minimum for being able to clearly demonstrate the size effect.

Because of the inevitable scatter, it would be desirable in the future to test specimens of broader size ranges.

3. Observed Size Effect

The effect of structure size on the nominal strength of geometrically similar quasibrittle materials generally follows the approximate size effect law[(3),(4)]:

$$\sigma_N = \frac{Bf_u}{\sqrt{1+\beta}} \qquad \beta = \frac{D}{D_0} \qquad (1)$$

where,

β = relative structure size
$\sigma_N = \frac{c_N P_{max}}{bD}$ = nominal strength
P_{max} = maximum load
D = characteristic dimension (size) of structure
b = width of structure in the third dimension (only two-dimensional similarity is considered here)

c_N = chosen coefficient introduced for convenience, (for example to make σ_N coincide with the maximum stress in the specimen calculated by bending theory)

D_0 = constant depending on both fracture process zone size and specimen geometry

B = constant characterizing the solution according to plastic limit analysis based on the strength concept

f_u = reference strength of the material (laminate), introduced to make B dimensionless

Equation 1 is valid not only for the two-dimensional similarity considered here (b =constant) but also for three dimensional similarity provided that there is no thickness effect on fracture properties.

To determine the parameters of the size effect law by regression analysis of experimental data, we define the following

$$D = X$$
$$\sigma_N = \frac{1}{\sqrt{Y}}$$
$$Bf_u = \frac{1}{\sqrt{A}} \qquad (2)$$
$$D_0 = \frac{A}{C} = \frac{1}{C(Bf_u)^2}$$

Then, the size effect law of Equation 1 is expressed in the form

$$Y = A + CX \qquad (3)$$

A linear regression analysis was conducted by plotting Y versus X in Figure 8 for the obtained experimental data. The parameters of the size effect law were obtained from the slope C and the vertical intercept A of these plots as follows:

D_0 = 41.7 mm (1.642 in.)

Bf_u = 0.440 GPa (63.82 ksi)

Subsequently, the resulting size effect was represented by plotting $\log(\sigma_N / Bf_u)$ versus $\log(D/D_0)$ in Figure 7. This size effect plot represents a transition from the strength criterion (plastic limit analysis) characterized by a horizontal asymptote, to an asymptote of slope -0.5, representing linear elastic fracture mechanics (LEFM).

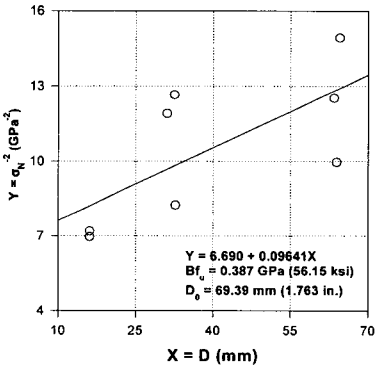

Fig. 8 Linear regression for determination of size effect parameters

The intersection of the two asymptotes corresponds to $D = D_0$, called the transitional size.

The test results in Figure 7 shows that: (1) the failure of fiber composite laminates containing traction-free cracks (or notches) exhibits a significant size effect, and that (2) the size effect represents a gradual transition with increasing size from the strength criterion to linear elastic fracture mechanics, as described by the size effect law, Equation 1. The foregoing conclusion is verified on the

average, as the mean statistical trend. These conclusions ought to be taken into account in all design situations and safety evaluations where a large traction-free crack can grow in a stable manner prior to failure. Especially, these conclusions are important for extrapolation from small-scale laboratory tests to real size aerospace or other structures. The strength theory, which does not account for size effect, is inadequate for these applications.

4. Identification of Material Fracture Characteristics from Measured Size Effect

The size effect law, Equation 1, for quasi-brittle fracture can also be expressed in terms of the nondimensionalized energy release rate $g(\alpha)$[6, 9, 10]:

$$\sigma_N = c_n \sqrt{\frac{EG_f}{g'(\alpha_0)c_f + g'(\alpha_0)D}} \tag{4}$$

where,

G_f = fracture energy release rate of the material

c_f = constant representing the effective length of fracture process zone defined by extrapolation to infinite size

α_0 = a_0 / D (initial value of $\alpha = a / D$)

a_0 = length of notch or initial traction-free crack

a = crack length

$g(\alpha)$ = $G(\alpha)Eb(D/P)^2$ (dimensionless energy release rate)

$G(\alpha)$ = energy release rate per unit width of crack front edge calculated by linear fracture mechanics (LEFM)

$g'(\alpha)$ = $dg(\alpha)/d\alpha$

E = Young's modulus

b = thickness

D = characteristic structure size taken as specimen width for a single-edge-notch specimen[8]

By matching Equations 4 and 1, one obtains[8, 9, 10]:

$$G_f = \frac{(Bf_u)^2}{c_n^2 E} \cdot D_0 g(\alpha_0)$$
$$c_f = \frac{g(\alpha_0)}{g'(\alpha_0)} D_0 \tag{5}$$

As the only possible unambiguous definition, the fracture energy is defined as the energy required for fracture propagation in a specimen of theoretically infinite size[11]. According to this definition, the fracture energy is independent of both the shape and size of the specimen because in a specimen of infinite size the fracture process zone occupies an infinitely small portion of the specimen volume and can be considered as a point, which means that linear elastic fracture mechanics can be applied.

To determine the material fracture characteristic on the basis of Equation 5, the expressions for the stress intensity factor K_I available for isotropic specimens[15] have been used. According to LEFM,

$$K_I = \sigma\sqrt{\pi b a}F(\alpha) \qquad \alpha = \frac{a}{D} \tag{6}$$

where,

$\sigma = \sigma_N$

(average stress in the laminate strip)

F = a function of the variable α

The unidirectional laminate is not isotropic but orthotropic. The energy release rate and the stress intensity factor for orthotropic specimens of the present geometry have recently been solved by Bao et al.[1]. Their solution uses elastic parameters defined as:

$$\rho = \frac{\sqrt{E_x E_y}}{2G_{xy}} - \sqrt{\nu_{xy}\nu_{yx}} \qquad \lambda = \frac{E_y}{E_x} \tag{7}$$

E_x, E_y, G_{xy}, ν_{xy}, ν_{yx} are the elastic constants of the orthotropic material referred to its principal material axes x and y, which can be obtained from the lamina properties from the manufacturer.

The stress intensity factor can be written as:

$$K_I = \sigma\sqrt{\pi b\alpha}\, Y(\rho) F(\alpha) \tag{8}$$

where,

$$Y(\rho) = [1 + 0.1(\rho - 1) - 0.016(\rho - 1)^2 + 0.002(\rho - 1)^3]\left(\frac{\rho + 1}{2}\right)^{-1/4}$$

$F(\alpha)$ = the same function of the relative crack length α = a/b as for isotropic materials

$Y(\rho)$ = material constant depending on orthotropy parameter

The energy release rate for an orthotropic material is:

$$G(\alpha) = \sqrt{\frac{1+\rho}{2E_x E_y\sqrt{\lambda}}}\, K_I{}^2 \tag{9}$$

Bringing Equation 8 into 9, one can write $G(\alpha)$ in the same form as for the isotropic materials:

$$G(\alpha) = \frac{K_I{}^2}{E^*} = \frac{\sigma^2 b\pi\alpha}{E^*} F^2(\alpha) = \left(\frac{P}{bD}\right)^2 \frac{b}{E^*} g(\alpha) \tag{10}$$

where,

$$E^* = \frac{1}{Y^2(\rho)}\sqrt{\frac{2E_x E_y\sqrt{\lambda}}{1+\rho}}$$

$g(\alpha)$ = nondimensionalized energy release rate defined before

By virtue of Equation 9, we can treat the orthotropic material fracture characteristics in the same way as the isotropic ones if we replace E by the equivalent Young's modulus E^* (E^*= 2.15 Msi =14.84 GPa for the uniaxial specimen).

For the single-edge notched specimen[15]:

$$F(\alpha) = 1.122 - 0.231\alpha + 10.55\alpha^2 - 21.71\alpha^3 + 30.38\alpha^4 \tag{11}$$

Noting that $K_I{}^2 = GE$ where G = energy release rate and E = Young's modulus, we have $g(\alpha) = \pi\alpha F(\alpha)^2$.

Thus, for the single-edge notched specimens:

$$g(\alpha) = \pi\alpha[1.122 - 0.231\alpha + 10.55\alpha^2 - 21.71\alpha^3 + 30.38\alpha^4]^2 \tag{12}$$

$$g'(\alpha) = \pi[1.259 - 1.037\alpha + 71.18\alpha^2 - 214.4\alpha^3 + 947.5\alpha^4 - 2832.7\alpha^5 + 7786.4\alpha^6 - 10552.8\alpha^7 + 7383.6\alpha^8]^2$$

where,

$$\alpha = 0.3$$

we have

$$g(0.3)=2.604,\ g'(0.3)=29.03.$$

Thus, the for single-edge notched unidirectional laminates we obtain from Equation 5 the effective fracture characteristics:

$$G_f = 0.796\ (\mathrm{MJ/m})^2\ (5.49\ \mathrm{ksi^*in})$$
$$c_f = 6.224\ \mathrm{mm}\ (0.158\ \mathrm{in})$$

Because of orthotropy, these values are valid only for fracture along the principal x-direction of orthotropy.

5. Conclusions

(1) Transverse slanting of the notch in test specimens of PEEK laminate can achieve pure out-of-plane kink band failure, not contaminated by shear of splitting cracks.

(2) The experimental results presented show that the nominal strength of geometrically similar notched specimens failing purely by kink band propagation exhibits a strong (non-statistical) size effect.

(3) The size effect governed by energy release is observed. The size effect law for notched specimens permits easy identification of the fracture energy of the kink band and the length of the fracture process zone at the front of the band solely by the measurements of maximum loads.

(4) The test results agree with the approximate size effect law proposed by Bazant(2),(3),(5). But the high scatter of test data, combined with a limited size range and scope, prevents regarding the test results as a proof of validity.

(5) The size effect law for notched specimens permits easy identification of the fracture energy of the kink band and the length of the fracture process zone at the front of the band solely by the measurements of maximum loads.

(6) The results suggest that the current strength criteria based design practice should be revised,

References

1. Bao, G., Ho, S., Suo, Z., and Fan, B.(1992). "The role of material orthotropy in fracture specimens for composites." Int. J. Solid Strct., 29 (9), 1105-1116.
2. Bazant, Z.P. (1983). "Fracture in concrete and reinforced concrete," Preprints, IUTAM Prager Symposium on Mech. of Geomaterials: Rocks, Conc., Soils, ed. by Z.P. Bazant, Northwestern University, Evanston, Illinois, 281-316.
3. Bazant, Z.P. (1984). "Size effect in blunt fracture: concrete, rock, and metal." J. of Engrg. Mech. ASCE, 110, 518-535.
4. Bazant, Z.P. (1993). "Scaling laws in mechanics of failure." J. of Engrg. Mech. ASCE, 119 (9), 1828-1844.
5. Bazant, Z.P. (1997). "Scaling of quasibrittle fracture: Asymptotic analysis." Int. J. of Fracture, 83 (1), 19-40.
6. Bazant, Z.P., and Cedolin, L. (1991). Stability of structures: Elastic, Inelastic, Fracture and Damage Theories, Oxford University Press, New York.
7. Bazant, Z.P., Daniel, I.M., and Li, Z. (1996). "Size effect and fracture characteristics of composite laminates." J. of Engrg. Materials and Technology ASME, 118 (3), 317-324.
8. Bazant, Z.P., Gettu, R., and Kazemi, M.T.

(1991). "Identification of nonlinear fracture properties from size effect tests and structural analysis based on geometry-dependent R-curves." Int. J. of Rock Mech., Mining Science & Geomechanical Abstracts, 28(1), 43-51.

9. Bazant, Z.P., and Kazemi, M.T. (1990a). "Determination of fracture energy, process zone length and brittleness number from size effect, with application to rock and concrete." Int. J. of Fracture, 44, 111-131.
10. Bazant, Z.P., and Kazemi, M.T. (1990). "Size effect in fracture of ceramics and its use to determine the fracture energy and effective process zone length." J. of merican Ceramic Society, 73 (7), 1841-1853.
11. Budianski, B. (1983). "Micromechanics." Computers and Strct., 16 (No. 1-4), 3-12.
12. Fleck, N.A., Sutcliffe, M.P.F., Sivashanker, S., and Xin, X.J. (1996). "Compressive R-curve of a carbon fiber-epoxy matrix composite." Composites Part B-Engrg., 27 (6), 531-541.
13. Fleck, N.A. (1997). " Compressive failure of fiber composites." Advances in Appl. Mech., 33,3-117.2
14. Tada, H., Paris, P.C., and Irwin, G.R. (1985). Stress Analysis of Cracks Handbook, Second Edition, Paris Productions Inc., Missouri.